Materials Sciences and Applications, 2014, 5, 459-466
Published Online May 2014 in SciRes. http://www.scirp.org/journal/msa
http://dx.doi.org/10.4236/msa.2014.57049

Scientific Research

Titanium Oxide Nanorods pH Sensors: Comparison between Voltammetry and Extended Gate Field Effect Transistor Measurements

Elidia Maria Guerra[1*], Marcelo Mulato[2]

[1]Department of Chemistry, Biotechnology and Bioprocess Engineering, Federal University of São João Del Rei, Ouro Branco, Brazil
[2]Department of Physics, São Paulo University, Ribeirão Preto, Brazil
Email: *elidiaguerra@ufsj.edu.br

Received 6 February 2014; revised 19 March 2014; accepted 7 April 2014

Abstract

In recent years there has increased interest in the characterization of titanium oxide nanorods for application in analytical devices. The titanium oxide nanorods (NRTiO) were obtained by hydrothermal reaction with a NaOH solution heated in the autoclave at 150˚C for up to 50 h. Experimental data indicate that the prepared nanorods consist of anatase and rutile phases, with a possible interlayer structure. The NRTiO was investigated as pH sensor in the pH range 2 - 12, and the extended gate field effect transistor (EGFET) configuration presented a sensitivity of 49.6 mV/pH. Voltammetric data showed a sensitivity of 47.8 mV/pH. These results indicate that the material is a promising candidate for applications as an EGFET-pH sensor and as a disposable biosensor in the future.

Keywords

Titanium Oxide Nanorods, pH Sensors, EGFET, Voltammetry

1. Introduction

It is well known that the structure of a material influences its final properties, *i.e.*, its characteristics depend on its structure. Many kinds of nanodimensional materials like nanowires, nanorods, nanofibers, and nanotubes

*Corresponding author.

How to cite this paper: Guerra, E.M. and Mulato, M. (2014) Titanium Oxide Nanorods pH Sensors: Comparison between Voltammetry and Extended Gate Field Effect Transistor Measurements. *Materials Sciences and Applications*, **5**, 459-466.
http://dx.doi.org/10.4236/msa.2014.57049

have been extensively studied [1]-[3]. However, to explore the novel applications of functional nanostructured materials remains a challenge. The extraordinary properties of some nanostructured materials make them attractive for the fabrication of novel analytical devices that have advantages over traditional ones, for instance, low cost, simple design, selectivity, miniaturization and improved sensitivity [4]. Besides, the demand for accurate, reliable, highly sensitive pH and biological sensors is increasing and these sensors are advancing rapidly due to their use in different areas, such as biochemistry and industrial processes [5]. Many different types of sensors have been architected, such as those based on field effect devices, because there is a high demand for specificity. Given the large demand for specific sensors, especially those based on field effect devices, many different types of materials have been developed as sensitive films or membranes. Furthermore, the determination of pH values is one of the most important tasks in analytical chemistry [6]. A development in pH measurement has been the introduction of the ion-sensitive field effect transistor (ISFET) technology as an alternative to the glass electrode [7] [8]. The flexible shape of the extended gate structure (EGFET) is another advantage of the latter type of transistors, whose better long-term stability stems from the fact that the ions present in the chemical environment are excluded from any region close to the FET gate insulator [9]. In addition, as in the case of ISFET sensors, there are several kinds of ion-sensing films and membranes that can be applied in the pH-sensing dielectric layers of pH-EGFET, such as ruthenium oxide [10] carbon nanotubes [11], SnO_2 [12] [13], ZnO [14], vanadium oxide [15], the V_2O_5 xerogel [16], vanadium/tungsten mixed oxides [17] [18]. In the search for another alternative of ion-sensing membranes for use in pH sensors, one can point out the titanium oxide nanorods (NRTiO), which displays useful chemical, optical, and electronic properties [19]-[21], and has been synthesized in nanosized configuration such as nanoparticles, nanowires, nanotubes, nanofibers, etc. [22] [23]. Besides, the NRTiO is nontoxic, biocompatible and environmentally safe, and it should offer large surface area compared with nanoparticles [24]-[29].

As described in the literature [12] [15] [16], the EGFET consists of two parts: the sensitive part is composed of a NRTiO immobilized on the substrate, and the system is completed with a commercial MOSFET CD-4007UB. This structure is easily constructed and has a lot of advantages compared with the ISFET, since it does not require the fabrication of the MOSFET.

The aim of this work is to fabricate titanium oxide nanorods, to explore the interaction of the ion-sensitive membrane with charges in solution, to find out the sensor sensitivity, and to verify its suitability as an EGFET-pH sensor. In addition to its electrical response as a pH sensor, the NRTiO material was also characterized by several techniques.

2. Experiment

The NRTiO was synthesized by the hydrolysis method, using 1.0 g of commercial titania (TiO_2) nanoparticle powder (Aldrich) as the starting material. In a typical hydrolysis experiment, the TiO_2 powder was processed in alkali solutions, such as NaOH (10 mol/L, 80 mL) using an autoclave, at a temperature of 150˚C, for time scales up to 50 h. During hydrolysis, titania nanoparticles were converted into titanate nanorods. The product was neutralized, followed by filtration and drying under atmospheric conditions [26] [29].

The X-ray diffraction (XRD) data were recorded on a SIEMENS D5005 diffractometer using a graphite monochromator and the CuK_α emission line (1.541 Å, 40 kV, 40 mA). To this end, samples in the film form deposited onto a glass plate were employed, and the data were collected at room temperature over the range $2^\circ \le 2\theta \le 50^\circ$, with a resolution of 0.020˚.

Fourier-transform infrared spectra (FTIR) were recorded from 4000 to 400 cm^{-1} on a Bomem MB 100 spectrometer. The samples were dispersed in KBr and pressed into pellets.

Scanning electron microscopy (SEM) was carried out on a ZEISS microscope EVO 50 model operating at 20 kV. A thin gold coating (≈20 Å) was applied to the sample using a Sputter Coater——Balzers SCD 050.

Voltammograms were measured using an AUTOLAB (EcoChemie) model PGSTAT30 (GPES/FRA) potentiostat/galvanostat interfaced with a computer. The conventional electrode arrangement was used, which consisted of glassy carbon as the working electrode, a platinum wire auxiliary electrode, and a saturated calomel electrode (SCE) as reference. The TiO_2 nanorod was deposited on the electrode surface, approximately 5 µL of the powder and dried at room temperature (24˚C). The supporting electrolyte was a buffer solution from pH 2 to 12. The voltammograms at different pHs were obtained at a potential scanning speed of 10 $mV{\cdot}s^{-1}$. All the experiments were carried out in deoxigenated solutions by bubbling N_2, at room temperature.

The electrical response of the EGFET sensor was measured using solutions of various pH values, and the

curves were obtained by an Agilent 34970A parameter analyzer. The electrode containing the sensing film was dipped into the buffer solution at room temperature for 5 minutes prior to the electrical measurement.

3. Results and Discussion

Figure 1 shows XRD patterns of the NRTiO. It is clear that the formation of anatase and rutile phases took place. The strongest peaks observed for the anatase and rutile phases were (101) $2\theta = 25.3^{\circ}$ and (110) $2\theta = 29.4^{\circ}$, respectively, indicating that NRTiO presents a crystalline structure. The presence of the typical diffraction peaks (101) in the XRD patterns of the NRTiO indicates a *d*-spacing of 0.35 nm. It has been reported that NRTiO presents a structure containing a separation between neighboring sheets surfaces, *i.e.*, the interspacing planes about 0.3784 nm [30]. Based on this observation, it is possible to estimate, from **Figure 1**, that the nanorod formation can be occurring. Broad and low intensity peaks suggest that the anatase and rutile phases may also contain an amorphous TiO_2 phase [31]. Concerning the presence of the anatase phase, the structure is bodycentered-tetragonal [30].

The weight percent of the anatase (W_A) and rutile (W_R) phases in the as-synthesized samples was calculated from the XRD patterns using Equations (1) and (2), as follows [32]:

$$W_R = \frac{1}{1+0.8\left(I_A/I_R\right)} \times 100 \tag{1}$$

$$W_A = 100 - W_R \tag{2}$$

where I_A and I_R are the integrated intensity of the (101) reflection of the anatase phase and the (110) reflection of the rutile phase, respectively. The phase composition of the sample was estimated Equations (1) and (2), and the result was $W_R = 76\%$ and $W_A = 24\%$.

The NRTiO was also characterized by FTIR between 4000 and 400 cm^{-1} and the results are presented in **Figure 2**. The FTIR spectrum of NRTiO displays broad, intense bands around 3300, 1634, and 1354 cm^{-1}, as well as a low intensity band at 902 cm^{-1}. The broad and intense band located around 3400 - 3000 cm^{-1} can be ascribed to OH stretching vibrations. This band indicates the presence of hydroxyl groups and huge amount of water molecules in the surface and interlayer space. The vibration around 1634 cm^{-1} also confirms the presence of water and can be assigned to H-O-H bending vibrations. The band around 902 cm^{-1} (inseted in **Figure 2**) represents the stretching vibration of short Ti-O bonds involving nonbridging oxygen probably coordinated with sodium ions. On the basis of the FTIR results, one can infer that the nanorods contain huge amounts of water and sodium ions present in the sample and, possibly, they are not only physically adsorbed to material, but they can also belong to the lattice [33]. When the IR spectrum of the nanorods was compared with those reported in the literature [33]-[35], the observed set of bands and the spectral features agree fairly well.

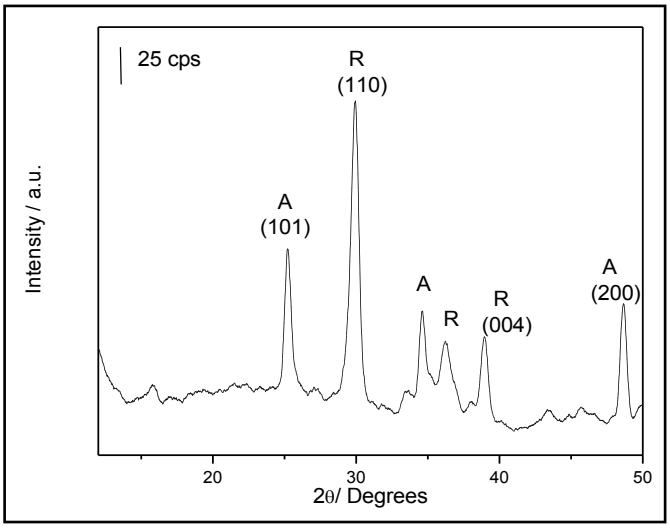

Figure 1. X-ray diffraction patterns of NRTiO.

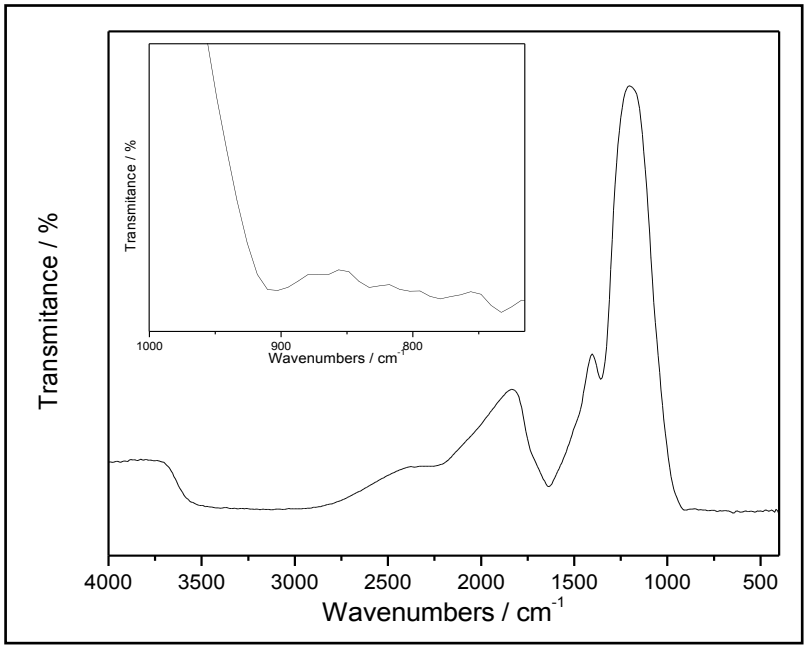

Figure 2. FTIR spectra of NRTiO.

The SEM image of the NRTiO is shown in **Figure 3**. As described in the literature [36], the commercial TiO_2 powder particles, used as starting material, are nearly spherical in shape and have a reasonably uniform size. However, after the hydrothermal synthesis in the presence of sodium hydroxide (NaOH), these particles undergo a delaminating process due to the attack of excess sodium cations, thus leading to two-dimensional nanosheets. The SEM results indicate that the nanorods were completely transformed into numerous stacking of wireshaped nanoparticles or into a connected nanostructure. Furthermore, as observed in **Figure 3**, the average size of these stacking of nanorods is 70 nm in diameter.

The sensitivity of the EGFET-pH sensor containing the NRTiO membrane can be obtained by measuring the relationship between drain current (I_D) and gate-source voltage (V_{GS}), which is shown in **Figure 4**.

From this figure, it is possible to note that there is a clear shift toward higher voltages with increasing pH values. **Figure 5** was produced from the data in **Figure 4** and the sensitivity was estimated using I_D = 400 μA at a V_{DS} of 0.3 V. On the basis of this I_D value, the sensitivity was 49.6 mV/pH. A variation of 10% in I_D leads to only 1.5% variation in sensitivity (in the range between 350 and 450 μA). As a result, the average sensitivity is very close to the theoretical limit of 59.2 mV/pH [37]. **Figure 5** shows that the EGFET exhibits good linearity, giving evidence of a constant behavior independent of the pH values.

Changes in the pH of the solution can alter the concentration of one of the species involved in the reaction, thus resulting in a shift in the redox potential. Voltammetrics studies were carried out to examine the pH dependence. **Figure 6** shows a number of voltammograms as a function of pH, in buffered electrolytes.

The cathodic peak region was selected, in order to ensure that the main features were preserved and to facilitate voltammogram analyses. **Figure 6** shows that the potential shifts to more negative values as the pH increases as predicted by the Nernst equation [38]. The pH dependence of potential (E) can also be seen in **Figure 7**, where E is plotted against the pH. The slope of the line is 47.8 mV/pH. From the Nernst equation, the slope of the plot of E vs. pH should be 59.2 mV/pH, which is very close to values obtained from EGFET study. Therefore, the EGFET-pH sensor based on titanium oxide nanorods is a promising set-up and it might be suitable as a device for use in disposable sensors.

As a sensing film on a pH-EGFET configuration, the NRTiO material demonstrated a linear behavior and a high sensitivity (49.6 mV/pH) for the pH range 2 - 12, a value 16% below the theoretical limit (59.2 mV/pH). The sensitivity was also studied by cyclic voltammetry, which led to a value of 47.8 mV/pH. Both techniques give very close results. Therefore, these results suggest that the material is a good candidate as pH sensor and may be even further employed as a biosensor for urea and glucose detection.

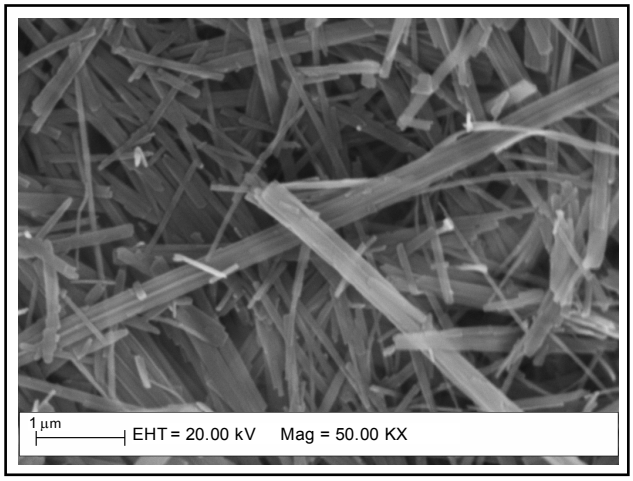

Figure 3. SEM image of NRTiO.

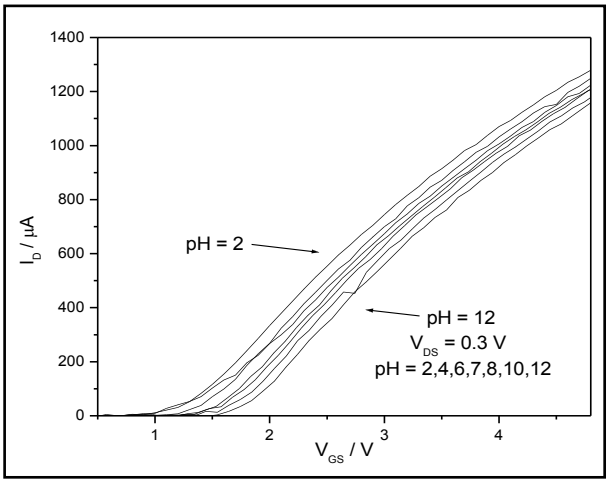

Figure 4. Response of a NRTiO-EGFET sensor in the linear region when immersed into solutions with pH values ranging from 2 to 12.

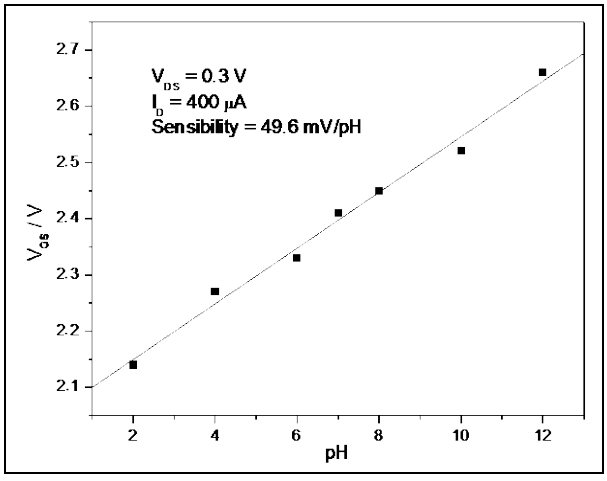

Figure 5. Sensitivity of the NRTiO-EGFET pH sensor: saturation response from pH 2 up to pH 12 in the linear region.

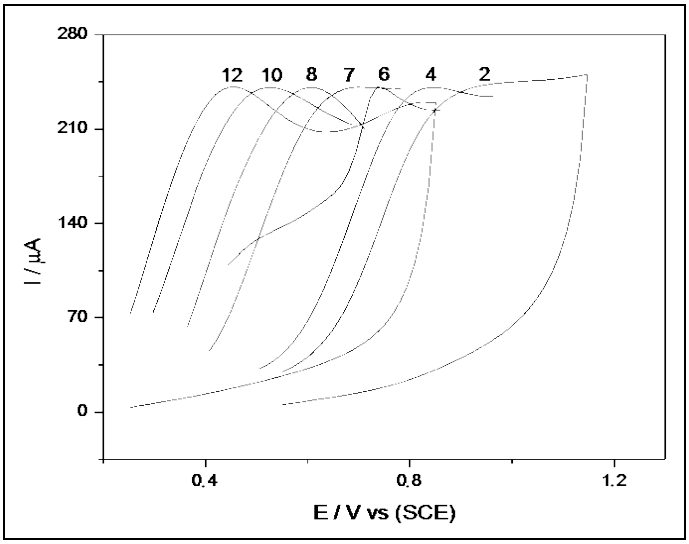

Figure 6. Voltammograms of NRTiO in buffer solution with pH values ranging from 2 to 12.

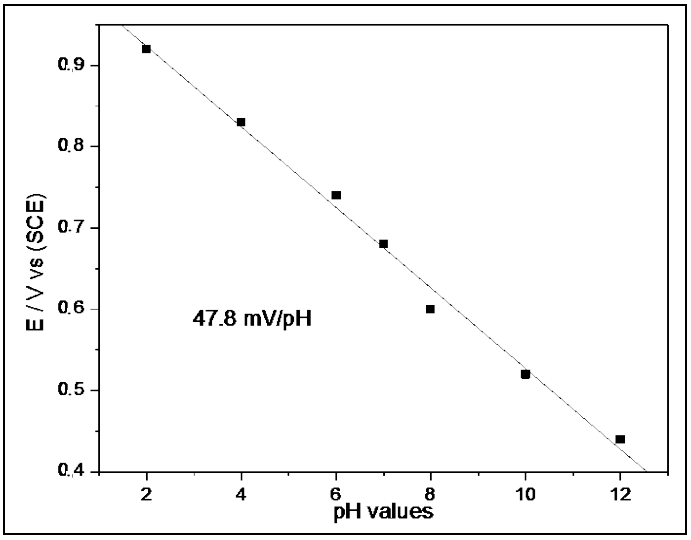

Figure 7. Potential range as a function of pH values for the NRTiO.

4. Conclusion

Titanium oxide nanorods were prepared in an autoclave at a temperature of 150˚C, for time scales up to 50 h. The X-ray diffraction data showed that the NRTiO presents anatase and rutile phases. The SEM shows the formation of numerous stacking of nanorods with an average diameter of 70 nm, thus indicating that the route employed was successful. As a sensing film on a pH-EGFET configuration, the NRTiO material demonstrated a linear behavior and a high sensitivity (49.6 mV/pH) for the pH range 2 - 12, a value 16% below the theoretical limit (59.2 mV/pH). The sensitivity was also studied by cyclic voltammetry, which led to a value of 47.8 mV/pH. Both techniques give very close results. Therefore, these results suggest that the material is a good candidate as a pH sensor and may be even further employed as a biosensor for urea and glucose detection.

Acknowledgements

The authors thank Prof. Herenilton P. Oliveira for allocation of his laboratory resources. This work was supported by FAPESP, FAPEMIG, CNPq and CAPES.

References

[1] Miao, Z., Xu, D., Ouyang, J., Guo, G., Zhao, X. and Tang, Y. (2002) Electrochemically Induced Sol-Gel Preparation of Single-Crystalline TiO_2 Nanowires. *Nano Letters*, **2**, 717-720. http://dx.doi.org/10.1021/nl025541w

[2] Limmer, S.J., Chou, T.P. and Cao, G.Z. (2004) A Study on the Growth of TiO_2 Nanorods Using Sol Electrophoresis. *Journal of Material Science*, **39**, 895-901. http://dx.doi.org/10.1023/B:JMSC.0000012919.21763.b2

[3] Kasuga, T., Hiramatsu, M., Hoson, A., Sekino, T. and Niihara, K. (1998) Formation of Titanium Oxide Nanotube. *Langmuir*, **14**, 3160-3163. http://dx.doi.org/10.1021/la9713816

[4] Liu, A., Wei, M., Honma, I. and Zhou, H. (2006) Biosensing Properties of Titanate Nanotube Films: Selective Detection of Dopamine in the Presence of Ascorbate and Uric Acid. *Advanced Functional Materials*, **16**, 371-376. http://dx.doi.org/10.1002/adfm.200500202

[5] Winquist, F. and Danielsson, B. (1990) Biosensors, A Practical Approach-Semiconductor Devices, Oxford University Press, Oxford.

[6] Vonau, W. and Guth, U. (2006) pH Monitoring: A Review. *Journal of Solid State Electrochemistry*, **10**, 746-752. http://dx.doi.org/10.1007/s10008-006-0120-4

[7] Miao, Y.Q., Chen, J.R., and Fang, K.M. (2005) New Technology for the Detection of pH. *Journal Biochemical and Biophysical Methods*, **63**, 1-9. http://dx.doi.org/10.1016/j.jbbm.2005.02.001

[8] Bergveld, P. (2003) Thirty Years of Isfetology: What Happened in the Past 30 Years and What May Happen in the Next 30 Years. S*ensors and Actuators B*: *Chemical*, **88**, 1-20. http://dx.doi.org/10.1016/S0925-4005(02)00301-5

[9] Chou, J.-C., Chiang, J.-L. and Wu, C.-L. (2005) pH and Procaine Sensing Characteristics of Extended-Gate Field-Effect Transistor Based on Indium Tin Oxide Glass. *Japanese Journal Applied Physics*, **44**, 4838-4842. http://dx.doi.org/10.1143/JJAP.44.4838

[10] Chou, J.C. and Tzeng, D.J. (2006) Study on the Characteristics of the Ruthenium Oxide pH Electrode. *Rare Metal Materials and Engineering*, **35**, 256-258.

[11] Silva, G.R., Matsubara, E.Y., Corio, P., Roselen, J.M. and Mulato, M. (2007) Carbon Felt/Carbon Nanotubes/Pani as pH Sensor. *Materials Research Society Proceedings*, *Spring Meeting*, **1018**, EE1410-EE1411. http://dx.doi.org/10.1557/PROC-1018-EE14-10

[12] Batista, P.D., Mulato, M., Graeff, C.F.D., Fernandez, F.J.R. and Marques, F.D. (2006) SnO_2 Extended Gate Field-Effect Transistor as pH Sensor. *Brazilian Journal of Physics*, **36**, 478-481. http://dx.doi.org/10.1590/S0103-97332006000300066

[13] Liao, H.-K., Chou, J.-C., Chung, W.-Y., Sun, T.-P. and Hsiung, S.-K. (1998) Study of Amorphous Tin Oxide Thin Films for ISFET Applications. *Sensors and Actuators B*: *Chemical*, **50**, 104-109. http://dx.doi.org/10.1016/S0925-4005(98)00162-2

[14] Batista, P.D. and Mulato, M. (2005) ZnO Extended-Gate Field-Effect Transistors as pH Sensors. *Applied Physics Letters*, **87**, 143508-143510. http://dx.doi.org/10.1063/1.2084319

[15] Guerra, E.M. and Mulato, M. (2009) Synthesis and Characterization of Vanadium Oxide/Hexadecylamine Membrane and Its Application as pH-EGFET Sensor. *Journal of Sol-Gel Science and Technology*, **52**, 315-320. http://dx.doi.org/10.1007/s10971-009-2062-7

[16] Guerra, E.M., Silva, G.R. and Mulato, M. (2009) Extended Gate Field Effect Transistor Using V_2O_5 Xerogel Sensing Membrane by Sol-Gel Method. *Solid State Science*, **11**, 456-460. http://dx.doi.org/10.1016/j.solidstatesciences.2008.07.014

[17] Guidelli, E.J., Guerra, E.M. and Mulato, M. (2011) Ion Sensing Properties of Vanadium/Tungsten Mixed Oxides. *Materials Chemistry and Physics*, **125**, 833-837. http://dx.doi.org/10.1016/j.matchemphys.2010.09.040

[18] Guidelli, E.J., Guerra, E.M. and Mulato, M. (2012) V_2O_5/WO_3 Mixed Oxide Films as pH-EGFET Sensor: Sequential Re-Usage and Fabrication Volume Analysis. *ECS Journal Solid State Science and Technology*, **1**, N39-N44. http://dx.doi.org/10.1149/2.007203jss

[19] Diebold, U. (2003) The Surface Science of Titanium Dioxide. *Surface Science Reports*, **48**, 53-229.

[20] Zhang, Y.X., Li, G.H., Jin, Y.X., Zhang, Y., Zhang, J. and Zhang, L.D. (2002) Hydrothermal Synthesis and Photoluminescence of TiO_2 Nanowires. *Chemical Physics Letters*, **365**, 300-304. http://dx.doi.org/10.1149/2.007203jss

[21] Ross, C. (2001) Patterned Magnetic Recording Media. *Annual Review of Materials Research*, **31**, 203-235. http://dx.doi.org/10.1146/annurev.matsci.31.1.203

[22] Li, W., Ni, C., Lin, H., Huang, C.P. and Shah, S.I. (2004) Size Dependence of Thermal Stability of TiO_2 Nanoparticles. *Journal of Applied Physics*, **96**, 6663-6668. http://dx.doi.org/10.1063/1.1807520

[23] Wang, J., Sun, J. and Bian, X. (2004) Preparation of Oriented TiO_2 Nanobelts by Microemulsion Technique. *Materials*

Science and Engineering: *A*, **379**, 7-10. http://dx.doi.org/10.1016/S0921-5093(03)00625-7

[24] Du, G.H., Chen, Q., Che, R.C., Yuan, Z.Y. and Peng, L.M. (2001) Preparation and Structure Analysis of Titanium Oxide Nanotubes. *Applied Physics Letters*, **79**, 3702-3704. http://dx.doi.org/10.1063/1.1423403

[25] Chen, Y.F., Lee, C.Y., Tao, Z.L., Yeng, M.Y. and Chiu, H.T. (2003) Titanium Disulfide Nanotubes as Hydrogen-Storage Materials. *Journal of the American Chemical Society*, **125**, 5284-5285. http://dx.doi.org/10.1021/ja034601c

[26] Chen, Y.F., Lee, C.Y., Yeng, M.Y. and Chiu, H.T. (2003) Preparing Titanium Oxide with Various Morphologies. *Materials Chemistry and Physics*, **81**, 39-44. http://dx.doi.org/10.1016/S0254-0584(03)00100-7

[27] Sander, M.S., Côté, M.J., Gu, W., Kile, B.M. and Tripp, C.P. (2004) Template-Assisted Fabrication of Dense, Aligned Arrays of Titania Nanotubes with Well-Controlled Dimensions on Substrates. *Advanced Materials*, **16**, 2052-2057. http://dx.doi.org/10.1002/adma.200400446

[28] Macák, J.M., Tsuchiya, H. and Schmuki, P. (2005) High-Aspect-Ratio TiO_2 Nanotubes by Anodization of Titanium. *Angewandte Chemie International Edition*, **44**, 2100-2102. http://dx.doi.org/10.1002/anie.200462459

[29] Mor, G.K., Shankar, K., Paulose, M., Varghese, O.K. and Grimes, C.A. (2005) Enhanced Photocleavage of Water Using Titania Nanotube Arrays. *Nano Letters*, **5**, 191-195. http://dx.doi.org/10.1021/nl048301k

[30] Yao, B.D., Chan, Y.F., Zhang, X.Y., Zhang, W.F., Yang, Z.Y. and Wang, N. (2003) Formation Mechanism of TiO_2 Nanotubes. *Applied Physics Letters*, **82**, 281-283. http://dx.doi.org/10.1063/1.1537518

[31] Juengsuwattananon, K., Jaroenworaluck, A., Panyathanmaporn, T., Jinawath, S. and Supothina, S. (2007) Effect of Water and Hydrolysis Catalyst on the Crystal Structure of Nanocrystalline TiO_2 Powders Prepared by Sol-Gel Method. *Physica Status Solidi* (*A*), **204**, 1751-1756. http://dx.doi.org/10.1002/pssa.200675328

[32] Spurr, R.A. and Myers, H. (1957) Quantitative Analysis of Anatase-Rutile Mixtures with an X-Ray Diffractometer. *Analytical Chemistry*, **29**, 760-762. http://dx.doi.org/10.1021/ac60125a006

[33] Qamar, M., Yoon, C.R., Oh, H.J., Lee, N.H., Park, K., Kim, D.H., Lee, K.S., Lee, W.J. and Kim, S.J. (2008) Preparation and Photocatalytic Activity of Nanotubes Obtained from Titanium Dioxide. *Catalysis Today*, **131**, 3-14. http://dx.doi.org/10.1016/j.cattod.2007.10.015

[34] Sauvet, A.L., Baliteau, S., Lopez, C. and Fabry, P. (2004) Synthesis and Characterization of Sodium Titanates $Na_2Ti_3O_7$ and $Na_2Ti_6O_{13}$. *Journal of Solid State Chemistry*, **177**, 4508-4515. http://dx.doi.org/10.1016/j.jssc.2004.09.008

[35] Marchand, R., Brohan, L. and Tournoux, M. (1980) TiO_2(B) a New Form of Titanium Dioxide and the Potassium Octatitanate $K_2Ti_8O_{17}$. *Materials Research Bulletin*, **15**, 1129-1133. http://dx.doi.org/10.1016/0025-5408(80)90076-8

[36] Godbole, V.P., Kim, Y.S., Kim, G.S., Dar, M.A. and Shin, H.S. (2006) Synthesis of Titanate Nanotubes and Its Processing by Different Methods. *Electrochimica Acta*, **52**, 1781-1787. http://dx.doi.org/10.1016/j.electacta.2005.12.058

[37] Temple-Boyer, P., Launay, J., Humenyuk, I., Do Conto, T., Martinez, A., Bériet, C. and Grisel, A. (2004) Study of Front-Side Connected Chemical Field Effect Transistor for Water Analysis. *Microelectronics Reliability*, **44**, 443-447. http://dx.doi.org/10.1016/j.microrel.2003.10.001

[38] Walczak, M.M., Dryer, D.A., Jacobson, D.D., Foss, M.G. and Flynn, N.T. (1997) pH Dependent Redox Couple: An Illustration of the Nernst Equation. *Journal Chemical Education*, **174**, 1195-1197. http://dx.doi.org/10.1021/ed074p1195